

**Complex scaling flows in the quench dynamics of interacting particles**Tilman Enss , Noel Cuadra Braatz , and Giacomo Gori *Institut für Theoretische Physik, Universität Heidelberg, 69120 Heidelberg, Germany*

(Received 21 March 2022; accepted 8 June 2022; published 8 July 2022)

Many-body systems driven out of equilibrium can exhibit scaling flows of the quantum state. For a sudden quench to resonant interactions between particles we construct a class of analytical scaling solutions for the time evolved wave function with a complex scale parameter. These solutions determine the exact dynamical scaling of observables such as the pair correlation function, the contact and the fidelity. We give explicit examples of the nonequilibrium dynamics for two trapped fermions or bosons quenched to unitarity, for ideal Bose polarons, and for resonantly interacting, Borromean three-body systems. These solutions reveal universal scaling properties of interacting many-body systems that arise from the buildup of correlations at short times after the quench.

DOI: [10.1103/PhysRevA.106.013308](https://doi.org/10.1103/PhysRevA.106.013308)**I. INTRODUCTION**

The quantum dynamics of strongly correlated many-body systems can often be described as fluid flow [1]. Near equilibrium, the slow relaxation of conserved charges and currents is governed by hydrodynamics [2,3]. Remarkably, even some situations far from equilibrium are well described by the equations of fluid dynamics, for instance the fast hydrodynamization observed in relativistic nuclear collisions [4]. Advances in ultracold quantum gas experiments now provide a new platform to explore far-from-equilibrium quantum dynamics in a controlled setting in the laboratory. In particular, recent experimental and theoretical studies have focused on the quench dynamics when strong or resonant interactions are suddenly switched on in bulk fermion [5,6], Fermi polaron [7,8], bulk boson [9–12], and Bose polaron [13–15] systems. Understanding the validity of fluid dynamics in these strongly correlated systems far from equilibrium has a wider impact for finding simpler effective descriptions of complex quantum dynamics.

A quench to strong interaction in a many-body system is generally a hard problem. However, at short times the dynamics is dominated by few-body correlations between nearby quantum particles [9,16] and similarly for an impurity quenched to strong interaction with a surrounding medium [7,14]. This universal short-time quantum dynamics applies equally to larger systems before the many-body timescale is reached. For longer times, instead, collective many-body excitations dominate and conformal symmetry can determine the long-time asymptotics [17].

In this work, we focus on the short-time dynamics in an extreme out-of-equilibrium setting and study few particles quenched from a noninteracting state to resonant contact interactions in a harmonic trapping potential. After the quench, an initially stationary quantum state becomes a highly excited state of the new Hamiltonian and can be represented as a large superposition of new eigenstates with a complicated time evolution. For two interacting particles, however, these

eigenstates are known and we find the analytical form of the time evolved wave function. From this solution we obtain the dynamical scaling of observables, in particular the full pair correlation function  $g^{(2)}(r, t)$ . For contact interactions in three dimensions it diverges as  $g^{(2)}(r, t) = C(t)/(4\pi r)^2$  for short distances  $r$  between the particles [18,19]. Starting from an initially noninteracting state, strong contact correlations build up linearly in time and the contact scales as  $C(t) \propto |\sin \omega_0 t|$  with trap frequency  $\omega_0$  [9]. We find that, due to this short-distance singularity, the fidelity has an anomalous time dependence  $1 - \gamma|t|^{3/2}$  for short times, as discussed in Sec. II.

The main goal of this work is to construct a class of analytical quench solutions in order to reveal universal scaling dynamics, generalizing the two-particle example above. We explain in Sec. III that this class of solutions for the global wave function has an analytical scaling form reminiscent of fluid flow. As a simple example, a quantum harmonic oscillator with time-dependent trapping potential can be transformed into a new time-varying coordinate system where the Hamiltonian is stationary [20–22]. The well-known solutions of the stationary harmonic oscillator can then be transformed back to the original coordinates where the dynamical wave function assumes a scaling form with a global scale parameter  $\lambda(t) > 0$ . In this work we show that also an interaction quench, which suddenly changes the Bethe-Peierls boundary condition of the wave function at short distance, can be brought into such a scaling form. However, we find that the quenched wave function is stationary in *complex* space and time coordinates, and the nonequilibrium quench dynamics in the original space-time coordinates is described by a scaling flow with a complex scale parameter  $\lambda(t) \in \mathbb{C}$ . Intriguingly, the complex time coordinate runs backward in real time, such that the quench evolution of an initial positive-energy state is given by the complex scaling flow of a *negative* energy stationary state. Expressing the quench dynamics as a scale transformation of a *single* stationary state constitutes a dramatic simplification compared with the generic time evolution of a highly excited state represented as a large superposition

of eigenstates. This is reminiscent of the complex scaling used to express a resonance not as an infinite superposition but as a single state of complex energy [23–25]. Our earlier explicit quench solution is an example of such a complex scaling flow.

After this general construction we apply the new class of solutions in Sec. IV to quench dynamics in few- and many-body systems, specifically to universal short-time scaling of observables, to quenched impurities in a Bose-Einstein condensate and to resonant, Borromean three-body systems. We conclude in Sec. V and discuss how strong few-body correlations constrain an effective fluid description of the strongly correlated quantum gas.

## II. INTERACTION QUENCH DYNAMICS

To set the stage we begin by deriving an analytical solution of quench dynamics in the traditional way, as a superposition of eigenstates of the Hamiltonian after the quench. In the next section this solution will be rederived as an instance of complex scaling flows.

Consider two distinguishable particles in a 3D harmonic trapping potential  $V(r) = (m/2)\omega_0^2 r^2$  with trap frequency  $\omega_0$ . The particles of mass  $m$  shall interact via an attractive contact interaction and are described by the Hamiltonian

$$H = \frac{p_1^2}{2m} + \frac{p_2^2}{2m} + \frac{m}{2}\omega_0^2(r_1^2 + r_2^2) + g\delta_{\text{reg}}^{(3)}(\mathbf{r}_1 - \mathbf{r}_2). \quad (1)$$

We recapitulate the spectrum and eigenstates found in Ref. [26]; in the following we compute the nonequilibrium dynamics after a change in interaction [27], which has similarities to the one-dimensional case [28].

The center-of-mass (c.m.) motion in (1) decouples from the relative motion, and the wave functions factorize as  $\Psi(\mathbf{C}, \mathbf{r}) = \psi^{\text{c.m.}}(\mathbf{C})\psi^{\text{rel}}(\mathbf{r})$  with center-of-mass coordinate  $\mathbf{C} = (\mathbf{r}_1 + \mathbf{r}_2)/2$  and relative coordinate  $\mathbf{r} = \mathbf{r}_1 - \mathbf{r}_2$ . In three dimensions, the contact interaction needs to be regularized, and we choose the Fermi pseudopotential  $\delta_{\text{reg}}^{(3)}(\mathbf{r}) = \delta^{(3)}(\mathbf{r})\partial_r \dots$  of strength  $g = 4\pi\hbar^2 a/m$ , which is fully characterized by the  $s$ -wave scattering length  $a$ . The interaction affects only the relative motion, and only the  $l = 0$  partial-wave component for a zero-range interaction. The contact pseudopotential then leads to the Bethe-Peierls boundary condition for the relative radial  $l = 0$  wave function as  $r \rightarrow 0$ ,

$$\psi^{\text{rel}}(r) = A\left(\frac{1}{r} - \frac{1}{a}\right) + O(r). \quad (2)$$

The eigenfunctions for generic  $a$  are Whittaker functions  $W_{a,b}(x)$  which decay sufficiently for  $r \rightarrow \infty$ ,

$$\psi_v^{\text{rel}}(r) = r^{-3/2}W_{E_v^{\text{rel}}/2, 1/4}(r^2/\ell^2), \quad (3)$$

up to normalization. We express lengths in units of the relative oscillator length  $\ell = \sqrt{\hbar/\mu\omega_0}$  for reduced mass  $\mu = m/2$  and energies in units of the oscillator energy  $\hbar\omega_0$ . The energy eigenvalues of relative motion are given by  $E_v^{\text{rel}} = 2\nu + 3/2$ , where  $\nu$  denotes the noninteger generalization of the principal quantum number of the harmonic oscillator wave function. The wave function (3) satisfies the boundary condition (2) if

$\nu$  is related to the scattering length  $a$  as [26]

$$\frac{\Gamma(-\nu)}{\Gamma(-\nu - \frac{1}{2})} = \frac{\Gamma(-\frac{E^{\text{rel}}}{2} + \frac{3}{4})}{\Gamma(-\frac{E^{\text{rel}}}{2} + \frac{1}{4})} = \frac{\ell}{2a}. \quad (4)$$

In the weakly interacting limit  $a \rightarrow 0^-$  with integer  $\nu = n = 0, 1, 2, \dots$  one recovers the spectrum  $E_{n,a \rightarrow 0^-} = 2n + 3/2$  of the breathing modes of the noninteracting harmonic oscillator. For larger values of  $1/a$  the energy levels decrease monotonically. A particularly interesting case is resonant scattering at  $1/a = 0$ , where the scattering amplitude reaches the maximum value consistent with unitarity and scale invariance is restored. At resonance (unitarity)  $\nu = n - 1/2$  takes half-integer values for  $n = 0, 1, 2, \dots$  and the eigenfunctions simplify to

$$\psi_{n,1/a=0}^{\text{rel}}(r) = \frac{e^{-r^2/2\ell^2} H_{2n}(r/\ell)}{\pi^{3/4} 2^n \sqrt{2(2n)!} \ell r} \quad (5)$$

with Hermite polynomials  $H_n(x)$ . The associated energy eigenvalues at resonance,

$$E_{n,1/a=0}^{\text{rel}} = 2n + 1/2, \quad (6)$$

are again *equally spaced* as in the noninteracting case, but shifted downward by one unit of  $\hbar\omega_0$ . Due to scale invariance at unitarity (the scattering length drops out as a length scale), an SO(2,1) symmetry emerges that generates the spectrum (6) at equidistant spacing  $2\hbar\omega_0$  [20,21,29–31].

The knowledge of eigenstates allows one to analytically compute the time evolution of the quantum gas after a quench from an ideal gas to unitarity. For definiteness we prepare the system in the harmonic oscillator ground state both for the center of mass and for the relative coordinate at  $a = 0^-$ ,

$$\psi_{0,a=0^-}^{\text{rel}}(\mathbf{r}) = \frac{e^{-r^2/2\ell^2}}{\pi^{3/4} \ell^{3/2}}. \quad (7)$$

When the interaction is suddenly quenched to unitarity at time  $t = 0$ , the wave function is projected onto the new eigenbasis of relative motion with coefficients

$$a_n = (\psi_{n,1/a=0}^{\text{rel}}, \psi_{0,a=0^-}^{\text{rel}}) = \frac{2^n}{\sqrt{2(2n)!}\Gamma(3/2 - n)}. \quad (8)$$

Computing  $\psi^{\text{rel}}(r, t) = \sum_{n=0}^{\infty} a_n e^{-itE_{n,1/a=0}^{\text{rel}}} \psi_{n,1/a=0}^{\text{rel}}(r)$  we find the full relative wave function after the quench to resonance as

$$\psi^{\text{rel}}(r, t) = \frac{e^{-3i\omega_0 t/2}}{\pi^{5/4} \ell^{3/2}} \left[ \frac{\sqrt{e^{2i\omega_0 t} - 1}}{r/\ell} e^{i(r^2/2\ell^2)\cot\omega_0 t} + \sqrt{\pi} e^{-r^2/2\ell^2} \operatorname{erf}\left(\frac{r/\ell}{\sqrt{e^{2i\omega_0 t} - 1}}\right) \right]. \quad (9)$$

The quench leaves the initial energy  $E^{\text{rel}} = \sum_n (2n + 1/2)|a_n|^2 = 3/2$  unchanged. This is expected from the dynamic sweep theorem because the expectation value of the contact operator vanishes in the Gaussian initial state, as we shall find below [18,19].

The pair correlation function of two particles at distance  $r$  and time  $t$ ,

$$g^{(2)}(r, t) = |\psi^{\text{rel}}(r, t)|^2, \quad (10)$$

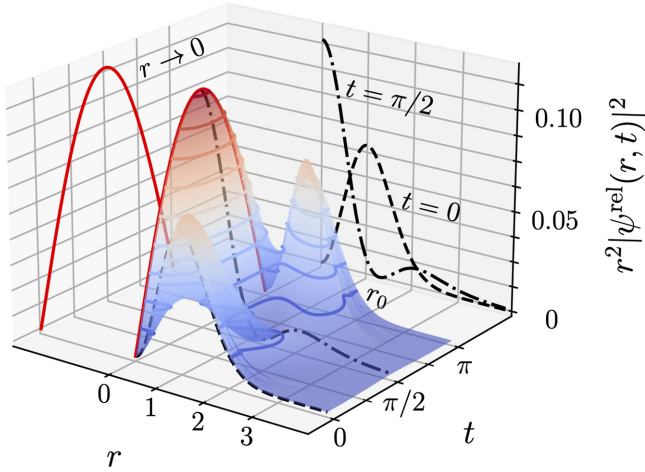


FIG. 1. Pair correlation function  $r^2 g^{(2)}(r, t) = r^2 |\psi^{\text{rel}}(r, t)|^2$  vs distance  $r$  at time  $t$  after a quench to unitarity ( $1/a = 0$ ), as given by Eq. (9). We give lengths in units of the trap length  $\ell$  and times in units of  $\omega_0^{-1}$ . The attractive interaction leads to a buildup of correlations at short distance  $r \rightarrow 0$ . At the same time, part of the correlation is pushed out so that an uncorrelated halo appears at  $r = r_0$  and  $\omega_0 t = \pi/2$  (see text). At  $r \rightarrow 0$  one can read off the contact  $C(t)$  (red solid line). Inside the trap the correlations are periodic in time with half the trap period. The black dashed and dash-dotted lines are the wave function at the beginning and halfway through the periodic motion, respectively.

is shown in Fig. 1. The initial Gaussian profile (weighted by  $r^2$ ) is spread out over the trap length  $r \simeq \ell$ . After the quench the attractive interaction pulls the particles together at  $r = 0$  and correlations start to grow at short distance. At short times, interference in the wave function (9) produces short-wavelength modulations that scramble the correlation at all distances. For longer times, however, the correlation function becomes smooth again. The harmonic confinement brings the wave function back to its initial state at half the trap period  $\omega_0 t = \pi$  and integer multiples; this is a consequence of scale invariance and the  $\text{SO}(2,1)$  symmetry [21]. Remarkably, at a quarter period  $\omega_0 t = \pi/2$  the correlation develops a node and splits into two disjoint regions at  $r = r_0 \approx 1.306\,930\ell$ , with the inner part attracted toward  $r = 0$  by the contact interaction, while the outer part is pushed farther out. Note that during the whole time evolution, the rms cloud size  $\langle r^2 \rangle(t) = \int d^3 r r^2 |\psi^{\text{rel}}(r)|^2 = (3/2)\ell^2$  remains constant even though the short-range correlations change dramatically.

In the short-distance limit the normalization (2) of the relative wave function is

$$A(t) = \lim_{r \rightarrow 0} r \psi^{\text{rel}}(r, t) = \frac{e^{-i\omega_0 t}}{\pi^{5/4} \ell^{1/2}} \sqrt{2i \sin \omega_0 t}. \quad (11)$$

This gives rise to the time evolution of the contact [9,18,19],

$$C(t) = \lim_{r \rightarrow 0} (4\pi r)^2 g^{(2)}(r, t) = |4\pi A(t)|^2 = \frac{32}{\sqrt{\pi} \ell} |\sin \omega_0 t|. \quad (12)$$

As shown in Fig. 2, immediately after the quench the contact  $C(t = 0) = 0$  vanishes as before the quench. As the interaction pulls together the particles, the contact grows linearly for short times. Eventually it reaches a maximum value of

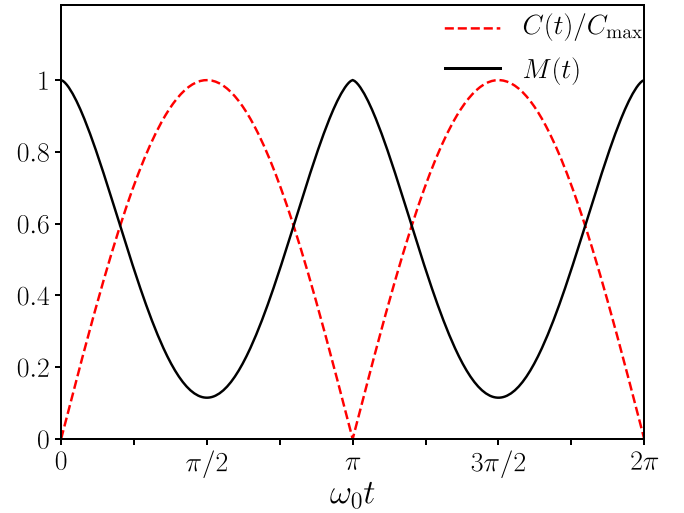


FIG. 2. Contact  $C(t)/C_{\text{max}}$  (dashed red line) at time  $t$  after a quench to unitarity ( $1/a = 0$ ), as given in Eq. (12). It rises linearly for short times and is periodic in time with half the trap period. The fidelity or Loschmidt echo  $M(t)$  (solid black line) in Eq. (13) is nonanalytic as  $1 - \gamma|t|^{3/2}$  for short times.

$C_{\text{max}} = 32/\sqrt{\pi} \ell$  at quarter period, before decreasing again as a  $\pi$ -periodic function in time.

While the contact is sensitive to the wave function at short distance, a measure of the evolution of the global quantum state is given by the fidelity between initial and time evolved states, or Loschmidt echo [27,28],

$$M(t) = |\langle \psi(0) | \psi(t) \rangle|^2 = \frac{4}{\pi^2} |\sqrt{e^{2i\omega_0 t} - 1} + \arcsin(e^{-i\omega_0 t})|^2. \quad (13)$$

For short times the Loschmidt echo is anomalously suppressed as  $M(t) = 1 - (8/3\pi)|\omega_0 t|^{3/2} + O(t^{5/2})$  and decreases faster than the usual  $t^2$  behavior which follows at intermediate times; this is due to the short-distance singularity of the contact interaction. The anomalously fast initial growth reflects the fast scrambling of the wave function manifest in the ripples of the pair correlation in Fig. 1 at short times. The same anomalous scaling is found for a quench in a bulk medium for times shorter than the many-body times scale [32]. Eventually, the Loschmidt echo reaches a minimum of  $M(\omega_0 t = \pi/2) = 4[\sqrt{2} - \ln(1 + \sqrt{2})]^2/\pi^2 \approx 0.115$  at quarter period and increases again to the next nonanalytic point at  $\omega_0 t = \pi$ , see Fig. 2.

### III. COMPLEX SCALING FLOWS

The exact quench dynamics in the harmonic trap (9) is a first example of a more general phenomenon and class of analytical quench solutions. In Eq. (9) the time evolved state is written as a large superposition of eigenstates of the quenched Hamiltonian which gives rise to a complicated transient behavior. We now show that the same wave function results from a *single stationary* state of the harmonic oscillator in a new coordinate system that is related to the original one by a global scale transformation. This dramatically simplifies the description of quench dynamics.

### A. Scaling dynamics

Scaling flows are a powerful way to describe the nonequilibrium time evolution of interacting quantum systems in the context of hydrodynamics [1,33], nonthermal fixed points [34] and trapped quantum gases [20,21,35]. As an example consider a two-dimensional quantum harmonic oscillator with time-dependent trapping frequency  $\omega(t)$ :

$$H(t) = \frac{\mathbf{p}^2}{2m} + \frac{m}{2}\omega^2(t)\mathbf{r}^2. \quad (14)$$

Initially the harmonic oscillator shall have a constant trapping frequency  $\omega(t) = \omega_0$  and wave function  $\tilde{\psi}(\mathbf{r}, t)$ . If the trapping frequency  $\omega(t)$  changes in time for  $t > 0$ , the wave function evolves as [21]

$$\psi(\mathbf{r}, t) = \frac{1}{\lambda(t)} \exp\left(\frac{im\mathbf{r}^2\dot{\lambda}(t)}{2\hbar\lambda(t)}\right) \tilde{\psi}(\boldsymbol{\rho}, \tau). \quad (15)$$

The original wave function  $\tilde{\psi}(\mathbf{r}, t)$  of the prequench Hamiltonian is evaluated at new space and time coordinates

$$\mathbf{r} \mapsto \boldsymbol{\rho} = \frac{\mathbf{r}}{\lambda(t)}, \quad t \mapsto \tau = \int_0^t \frac{dt'}{\lambda^2(t')} \quad (16)$$

in terms of a global, positive scale factor  $\lambda(t) > 0$ . The wave function  $\psi(\mathbf{r}, t > 0)$  after the quench (15) satisfies the Schrödinger equation for given time-dependent trapping frequency  $\omega(t > 0)$  if the scale factor evolves in time according to the Ermakov equation [20–22]

$$\ddot{\lambda} + \omega^2(t)\lambda = \frac{\omega_0^2}{\lambda^3}, \quad (17)$$

with initial conditions  $\lambda(0) = 1$ ,  $\dot{\lambda}(0) = 0$ . The  $1/\lambda$  term in (15) preserves the normalization of the wave function in two-dimensional space, while the phase factor that depends on space and time corresponds to a gauge transformation. In case  $\tilde{\psi}$  is a stationary state of the prequench Hamiltonian at energy  $E$ , one can replace  $\tilde{\psi}(\boldsymbol{\rho}, \tau(t)) = e^{-iE\tau(t)/\hbar} \tilde{\psi}(\boldsymbol{\rho}, 0)$ .

The time-dependent coordinate transformation (16) maps the driven oscillator into a stationary one in new space  $\boldsymbol{\rho}$  and time  $\tau$  coordinates [20–22]. Solutions  $\tilde{\psi}(\boldsymbol{\rho}, \tau)$  of the time-independent oscillator can then be transformed back to the original coordinates  $\mathbf{r}$ ,  $t$  to yield the nonequilibrium scaling solution (15). Remarkably, this scaling solution for a single driven oscillator extends to interacting many-body systems with scale invariant interactions that possess the  $SO(2,1)$  symmetry in a harmonic trap, such as the unitary Fermi gas [21,29] or the 2D quantum gas [20] up to the quantum scale anomaly [35–39]. It applies also to quantum statistical models where the quench dynamics can be mapped to that of harmonic oscillators, such as the spherical model [40].

An interaction quench as discussed above in Sec. II corresponds to a sudden change of the Bethe-Peierls boundary condition (2) for the relative  $s$ -wave function at  $r = 0$  from noninteracting (scattering length  $a = 0^-$ ) to resonant interactions ( $1/a = 0$ ). We demonstrate below that the ensuing quench dynamics is again given by a scaling solution of the form (15) but now with a *complex* scale factor that solves the Ermakov equation (17) with a different set of initial conditions. Remarkably, we find that the interaction quench dynamics is obtained as the scaling in complex space and time

of a *stationary* state  $\tilde{\psi}$ , albeit a different one from before, which yields closed analytical expressions for the nonequilibrium evolution. We now derive this for the generalized case of  $N$  interacting particles in a harmonic trapping potential.

### B. Trapped $N$ -particle systems

Consider a three-dimensional  $N$ -particle system in a harmonic trap. This is conveniently described in hyperspherical coordinates in terms of center of mass  $\mathbf{C}$ , hyperradius  $R$ , and a collection of hyperangles  $\Omega$  [30,41]. In the case of scale invariant interaction the wave function factorizes as

$$\Psi_{\text{trap}}(X) = \psi^{\text{c.m.}}(\mathbf{C})R^{-(3N-5)/2}F(R)\Phi(\Omega), \quad (18)$$

where  $X = (\mathbf{r}_1, \dots, \mathbf{r}_N)$  is the vector of all particle positions,  $\mathbf{C} = (1/N)\sum_k \mathbf{r}_k$  denotes the center-of-mass coordinate,  $R = [\sum_k (\mathbf{r}_k - \mathbf{C})^2]^{1/2}$  is the hyperradius, and  $\Omega$  denotes the hyperangles. The reason for choosing this coordinate system is that an  $N$ -body interaction affects only the  $R$  coordinate and turns it into a one-dimensional problem which can be solved analytically. The hyperangular wave function satisfies the Schrödinger equation

$$\left[ -\Delta_\Omega + \left(\frac{3N-5}{2}\right)^2 \right] \Phi(\Omega) = s^2 \Phi(\Omega), \quad (19)$$

with Laplacian  $\Delta_\Omega$  and energy eigenvalue  $s^2 \in \mathbb{R}$ . Since the harmonic confinement affects only the hyperradial and center-of-mass coordinates, the hyperangular solution determines also the relative wave function in free space,

$$\Psi_{\text{free}}(X) = R^{s-(3N-5)/2} \Phi(\Omega). \quad (20)$$

For noninteracting particles in three dimensions, the ground state has hyperangular eigenvalue  $s = (3N-5)/2$  such that  $s_{N=2} = 1/2$ ,  $s_{N=3} = 2$ , etc. For particles with resonant two-body interaction,  $s$  can take noninteger values, for instance  $s = 1.7727$  for  $N_\uparrow = 2$ ,  $N_\downarrow = 1$  fermions [41].

Given the value  $s$  of the hyperangular solution, the hyperradial wave function is found by solving the 2D radial Schrödinger equation with centrifugal barrier and oscillator confinement (from now on  $\hbar \equiv 1$ ),

$$-\frac{1}{2m} \left[ F'' + \frac{1}{R} F' \right] + \left( \frac{s^2}{2mR^2} + \frac{m}{2} \omega_0^2 R^2 \right) F(R) = E_{\text{rel}} F(R), \quad (21)$$

with the energy eigenvalue of relative motion  $E_{\text{rel}}$  and normalization  $\int_0^\infty dR R |F(R)|^2 = 1$ . For real  $s$  there is a tower of universal states ( $q \in \mathbb{N}_0$ )

$$F_q(R) = \sqrt{\frac{2(s+q)!}{q!s!^2}} \frac{1}{R} M_{E/2, s/2}(R^2) \quad (22)$$

$$= \sqrt{\frac{2q!}{(s+q)!}} R^s e^{-R^2/2} L_q^{(s)}(R^2), \quad (23)$$

with  $R$  in units of the oscillator length  $L = \sqrt{\hbar/m\omega_0}$ , while  $L_q^{(s)}(x)$  denotes associated Laguerre polynomials [30]. The energy eigenvalues  $E_{\text{rel}} = (1+s+2q)\hbar\omega_0$  are equally spaced within each tower of fixed  $s$ . For positive  $s > 0$  and small hyperradius  $R \rightarrow 0$  the radial ground-state wave function

scales as

$$F_0(R) \propto R^s [1 + O(R^2)]. \quad (24)$$

Note that both the hyperangular and the hyperradial Schrödinger equations depend only on  $s^2$  and admit two solutions  $s, -s$ . However, the sign change of  $s$  selects a solution with a different boundary condition for  $R \rightarrow 0$ , namely  $R^s$  vs  $R^{-s}$ , and a corresponding change of the ground-state energy from  $E = 1 + s$  to  $E = 1 - s$ . This generalizes the Bethe-Peierls boundary condition (2) to  $N$ -body interaction with a condition on the hyperradial wave function  $F(R)$  for small  $R \rightarrow 0$  ( $s > 0$ ) [30,42],

$$F(R) = A \left( R^{-s} - \text{sgn}(a) \frac{R^s}{|a|^{2s}} \right) + \dots \quad (25)$$

The  $R^s$  solution describes particles without  $N$ -body interaction (scattering length  $a \rightarrow 0$ ) where  $F(R)$  is bounded for  $R \rightarrow 0$ . The  $R^{-s}$  solution appears for  $N$ -body interaction of finite scattering length  $a \neq 0$ , and the  $R^s$  part disappears completely for resonant  $N$ -body interaction ( $a \rightarrow \infty$ ). For  $-s \leq -1$ , the normalization of the radial function  $F(R)$  can be formulated with a short-distance cutoff that excludes the repulsive core as done for  $p$ -wave and higher interactions [43,44].

Consider now a quench from a noninteracting trapped  $N$ -particle Bose gas to resonant  $N$ -body interactions. This results in a Borromean system with  $N$ -body but no  $(N - 1)$ -body or smaller interaction [45]. Initially, the noninteracting gas has  $s = (3N - 5)/2 > 0$ , and the hyperradial ground-state wave function

$$F_0(R) = \sqrt{\frac{2}{s!}} \frac{1}{R} M_{(1+s)/2, s/2}(R^2) = \sqrt{\frac{2}{s!}} R^s e^{-R^2/2} \quad (26)$$

is normalizable and has energy  $E_0 = 1 + s = \frac{3}{2}(N - 1)$  for the relative motion, which together with the center-of-mass energy  $E_{\text{c.m.}} = \frac{3}{2}$  yields the total energy of  $E_{\text{tot}} = \frac{3}{2}N$ . After the quench, the sign of  $s$  is flipped to  $-s$  [46] and the new resonant ground-state energy becomes

$$E_0^{\text{res}} = 1 - s. \quad (27)$$

The original wave function can be decomposed into a large superposition of the new eigenstates  $q \in \mathbb{N}_0$  with energies  $E_q^{\text{res}} = 1 - s + 2q$ , and the interference between the tower states results in the nonequilibrium quench dynamics as in Eq. (9), cf. Fig. 3.

### C. Analytical quench solution

We now construct the analytical solution of  $N$ -body quench dynamics. We start with the general scaling form of the wave function (15) with a complex scale parameter

$$\lambda(t) = \sqrt{e^{2i\omega_0 t} - 1} \in \mathbb{C}. \quad (28)$$

This solves the Ermakov equation for constant trapping frequency  $\omega_0$  but a vanishing scale parameter  $\lambda(t \rightarrow 0) = 0$  at the moment of the quench. The scaling transformation (16) relates the original Hamiltonian to a stationary one in new

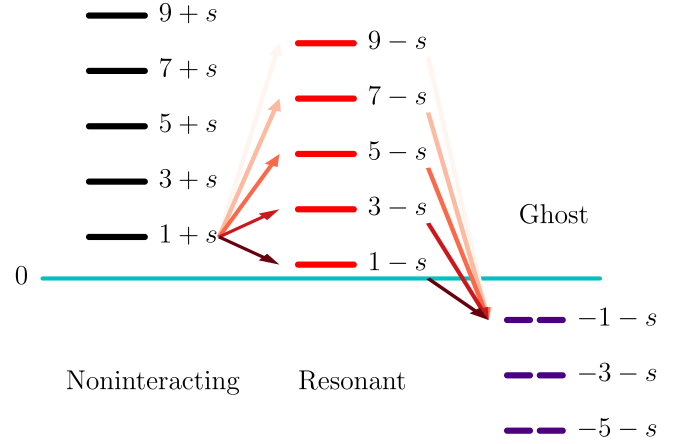


FIG. 3. Complex scaling inverts the arrow of time: the noninteracting initial state of energy  $1 + s$  (in the “Noninteracting” tower) can be represented either as an infinite superposition of postquench resonant states with energies  $1 - s + 2q$ ,  $q = 0, 1, 2, \dots$  (the “Resonant” tower), or equivalently as the complex scaling of a single stationary state of negative energy  $-1 - s$  (in the “Ghost” inverse tower) evolving backwards in time.

complex coordinates

$$\rho = R \sqrt{-\frac{1 + i \cot \omega_0 t}{2}}, \quad \tau = \int_\epsilon^t \frac{dt'}{\lambda^2(t')} = -t - i \ln \frac{\lambda(t)}{\lambda_\epsilon}, \quad (29)$$

with  $\lambda_\epsilon = \lambda(\epsilon) \sim \epsilon^{1/2}$  for short-time cutoff  $\epsilon \rightarrow 0$ . We observe that the proper time  $\tau$  runs backwards in real time  $t$ . Hence, the complex scaling inverts the energy of the stationary state  $\psi$ . Remarkably, there exists a negative-energy resonant state with  $q = -1$ ,

$$E_{-1}^{\text{res}} = 1 - s - 2 = -E_0, \quad (30)$$

whose energy is precisely the inverse of the prequench energy  $E_0$ . Therefore, a single stationary state is sufficient to describe the full quench dynamics of the initial positive-energy state  $E_0$  upon complex scaling. Figure 3 illustrates how complex scaling maps the negative energy state to precisely match the energy of the initial state. The corresponding state  $F_{-1}(\rho)$  results as the Whittaker function with negative second index  $-s/2 < 0$ ,

$$F_{-1}^{\text{res}}(\rho) = \mathcal{N} \frac{\lambda_\epsilon^{1+s}}{\Gamma(1-s)} \frac{1}{\rho} M_{-(1+s)/2, -s/2}(\rho^2) \quad (31)$$

$$= \sqrt{\frac{2}{s!}} \lambda_\epsilon^{1+s} \rho^s e^{\rho^2/2} [1 - \Gamma(-s, \rho^2)/\Gamma(-s)], \quad (32)$$

with the incomplete Gamma function  $\Gamma(-s, x)$ . By construction,  $F_{-1}^{\text{res}}(R)$  is not normalizable for real  $R \in \mathbb{R}$  because it is two levels below the oscillator ground state  $E_0^{\text{res}}$ . However, it becomes normalizable in complex space coordinate  $\rho = R/\lambda(t) \in \mathbb{C}$ . The complex scaling solution (15) with the stationary state  $F_{-1}^{\text{res}}(\rho)$  then reads

$$F(R, t) = \frac{\exp(-iE_{-1}^{\text{res}}\tau)}{\lambda(t)} \exp\left(\frac{iR^2\dot{\lambda}(t)}{2\lambda(t)}\right) F_{-1}^{\text{res}}(\rho). \quad (33)$$

Since the proper time  $\tau$  in (29) runs backwards in real time  $t$  the phase factor from the time evolution of the negative-energy stationary state  $E_{-1}^{\text{res}}$  turns into that of a positive-energy initial state  $E_0$  (whose energy remains unchanged by the quench) and an additional scale factor,

$$e^{-iE_{-1}^{\text{res}}\tau} = e^{-iE_0 t} \left( \frac{\lambda(t)}{\lambda_\varepsilon} \right)^{1+s}. \quad (34)$$

The  $\lambda_\varepsilon$  term in the global phase (34) compensates the corresponding term in the normalization in (31) to yield a finite result in the  $\varepsilon \rightarrow 0$  limit. Since  $\lambda$  is complex, the gauge factor changes not only the phase but also the amplitude, with complex exponent

$$\frac{iR^2 \dot{\lambda}}{2\lambda} = -\frac{R^2}{4}(1 - i \cot \omega_0 t) = \frac{1}{2} \bar{\rho}^2 \quad (35)$$

in terms of the complex-conjugate coordinate  $\bar{\rho}$ . Thus  $e^{(\bar{\rho}^2 + \rho^2)/2} = e^{-R^2/2}$  gives a pure amplitude factor while  $e^{(\bar{\rho}^2 - \rho^2)/2} = e^{iR^2 \cot(\omega_0 t)/2}$  is a pure phase. Collecting the terms in (33) we arrive at our main result, the analytical quench solution

$$F(R, t) = e^{-iE_0 t} F_0(R) \left[ 1 - \frac{\Gamma(-s, \frac{R^2}{e^{2i\omega_0 t} - 1})}{\Gamma(-s)} \right]. \quad (36)$$

It remains to be shown that the scaling solution (33), (36) satisfies (i) the Schrödinger equation (21) and (ii) the Bethe-Peierls boundary condition  $F(R, t) \sim R^{-s}$  for  $t > 0$ , and (iii) is continuous with the initial state (26) for  $t \rightarrow 0$ . In fact, (i) follows because the complex scale factor (28) satisfies the Ermakov equation (17) and  $F_{-1}^{\text{res}}(R)$  is a stationary solution of the Schrödinger equation, even though it has negative energy and is not normalizable. The boundary condition (ii) for  $t > 0$  follows from the short-distance expansion of (36) using  $\Gamma(-s, \rho^2 \rightarrow 0) = \rho^{-2s}/s + \dots$ . Continuity (iii) requires  $F(R, t \rightarrow 0) = F_0(R)$ : for short times  $\lambda^2 \rightarrow 2i\omega_0 t$  and  $\rho^2 = R^2/\lambda^2 \rightarrow -i\infty$  becomes large. In the  $t \rightarrow 0$  limit the incomplete Gamma function

$$\left| \Gamma\left(-s, \frac{R^2}{2it}\right) \right| \sim \left| \frac{t}{R^2} \right|^{1+s} \quad (37)$$

vanishes. We thus obtain the continuity of the wave function for short times,

$$F(R, t \rightarrow 0) = \sqrt{\frac{2}{s!}} R^s e^{-R^2/2} = F_0(R). \quad (38)$$

Hence, the full initial wave function with noninteracting  $R^s$  boundary condition is recovered for short times  $t \rightarrow 0$  or for distances  $R \gtrsim R_d(t) = \sqrt{2Dt}$  ( $|\rho| \gtrsim 1$ ) larger than the diffusion scale with quantum diffusivity  $D \simeq \hbar/m$  [47]. Complex scaling replaces this by the resonant  $R^{-s}$  boundary condition for longer times or shorter distances  $R \lesssim R_d(t)$ .

#### D. Example: Two particles in a harmonic trap

The general analytic solution (36) recovers our earlier result for  $N = 2$  particles derived in Sec. II. Indeed, with  $s = 1/2$  one has  $E_0 = 3/2$ ,  $E_0^{\text{res}} = 1/2$  and  $E_{-1}^{\text{res}} = -3/2 = -E_0$ .

The postquench stationary state at negative energy is

$$F_{-1}^{\text{res}}(\rho) = \frac{2\lambda_\varepsilon^{3/2}}{\pi^{3/4}} \rho^{-1/2} e^{-\rho^2/2} [1 + \sqrt{\pi} \rho e^{\rho^2} \text{erf}(\rho)], \quad (39)$$

while the quench solution reads

$$F(R, t) = e^{-iE_0 t} \frac{2R^{1/2}}{\pi^{3/4}} \left[ \frac{1}{\rho} e^{i(R^2/2) \cot \omega_0 t} + \sqrt{\pi} e^{-R^2/2} \text{erf} \rho \right].$$

We thus find the quenched 3D wave function  $\psi(r, t) = (4\pi r)^{-1/2} F(R/L = r/\ell, t)$ , in agreement with Eq. (9).

## IV. APPLICATIONS

From the analytical quench solution (36) it is now straightforward to obtain the dynamical scaling of observables after the quench.

### A. Dynamical scaling of observables

While the energy of the initial state remains unchanged after the quench, the density profile evolves in time. In particular, the  $N$ -body hyperradial correlation function ( $s > 0$ )

$$\begin{aligned} g^{(N)}(R, t) &= |F(R, t)|^2 = \frac{2}{s!} R^{2s} e^{-R^2} \left| 1 - \frac{\Gamma(-s, \rho^2)}{\Gamma(-s)} \right|^2 \\ &= C^{(N)}(t) R^{-2s} + O(R^{-2s+2}) \end{aligned} \quad (40)$$

manifests how the overall scale of the gas responds to a change in the  $N$ -body interaction. This is the  $N$ -body generalization of the pair correlation function (10) for  $N = 2$  and  $s = 1/2$ . Figure 1 illustrates how after the quench the inner part  $R \lesssim L$  is pulled in, while the outer part  $R \gtrsim L$  is pushed further out. Despite the internal motion, the average cloud size (virial)

$$\langle R^2 \rangle(t) = \int_0^\infty dR R^2 g^{(N)}(R, t) = (1+s)L^2 \quad (41)$$

remains constant after the quench for generic  $s$ , extending our result for  $s = 1/2$  below Eq. (10).

In the short-distance limit the  $N$ -body hyperradial correlations (40) are singular for resonant interaction as a consequence of the Bethe-Peierls boundary condition (25). The dynamical scaling of this singularity is given by the  $N$ -body contact parameter

$$\begin{aligned} C^{(N)}(t) &= \lim_{R \rightarrow 0} |R^s F(R, t)|^2 = \frac{2}{s! s^2} |\lambda(t)|^{4s} \\ &= \frac{2^{2s+1}}{s! s^2} |\sin \omega_0 t|^{2s}. \end{aligned} \quad (42)$$

As discussed above, for  $s \geq 1$  a short-distance cutoff  $R > R_c$  can be used and the contact is read off just outside the cutoff radius. The  $N$ -body contact is initially zero for an  $N$ -body noninteracting state and rises as  $|t|^{2s}$  for short times to reach a maximum value at quarter period  $\omega_0 t = \pi/2$ . This generalizes our earlier result (12) for the time-dependent contact of two particles with  $s = 1/2$ .

Finally, the wave-function overlap of the time evolved initial and quenched states deviates from unity as  $t^{1+s}$  for short

times,

$$\langle \psi_0(t) | \psi(t) \rangle = e^{iE_0 t} \int_0^\infty dR R F_0(R) F(R, t) \quad (43)$$

$$= 1 - \frac{\lambda^{2(1+s)} {}_2F_1(1, 1+s, 2+s, -\lambda^2)}{(1+s)!(-1-s)!} \quad (44)$$

$$= 1 - \frac{(2i\omega_0 t)^{1+s}}{(1+s)!(-1-s)!} + \dots,$$

with hypergeometric function  ${}_2F_1(a, b, c, x)$ . For  $s = 1/2$  this recovers the scaling of the Loschmidt echo for two particles [13].

### B. Many-body system in free space: Resonant impurity in an ideal Bose-Einstein condensate

The quench dynamics of a harmonically trapped gas straightforwardly includes the dynamics in free space by taking the limit of vanishing trap frequency  $\omega_0 \rightarrow 0$ . To see this, we include again units and find

$$\rho^2 = \frac{R^2 / (\hbar/m\omega_0) \xrightarrow{\omega_0 \rightarrow 0} mR^2}{e^{2i\omega_0 t} - 1} \rightarrow \frac{mR^2}{2i\hbar t}, \quad (45)$$

with  $\lambda(t) \approx \sqrt{2i\omega_0 t}$ , while  $\exp(-R^2/2L^2) \rightarrow 1$  in this limit. The analytical quench dynamics in free space is thus given by the wave function

$$F_{\text{free}}(R, t) = R^s \left( 1 - \frac{\Gamma(-s, mR^2/2i\hbar t)}{\Gamma(-s)} \right). \quad (46)$$

The exact quench evolution (46) applies directly to an ideal Bose-Einstein condensate (BEC) with a heavy impurity particle, which is suddenly quenched to resonant interaction with the surrounding condensate particles and thereby forms an ideal Bose polaron [14]. The condensate wave function  $\phi(r, t)$  at distance  $r$  from the impurity agrees with the relative wave function (9), (46) up to an overall normalization factor for  $N$  particles in the condensate, and we find

$$\phi(r, t) = \sqrt{N} \psi^{\text{rel}}(r, t) \xrightarrow{\omega_0 \rightarrow 0} \sqrt{\frac{N}{4\pi r}} F_{\text{free}}(r, t). \quad (47)$$

For a uniform BEC in the  $\omega_0 \rightarrow 0$  limit we thus obtain the quench solution

$$\phi(r, t) = \lim_{\omega_0 \rightarrow 0} \sqrt{\pi^{3/2} n \ell^3} \psi^{\text{rel}}(r, t) \quad (48)$$

$$= \sqrt{n} \left( \sqrt{\frac{2i\hbar t}{\pi m r^2}} e^{-mr^2/2i\hbar t} + \text{erf} \sqrt{\frac{mr^2}{2i\hbar t}} \right). \quad (49)$$

Here  $m = m_B$  denotes the reduced mass between a boson of mass  $m_B$  and the infinitely heavy impurity. This result reproduces the exact quench solution for the ideal Bose polaron in a uniform BEC derived recently in a continuum computation [14].

### C. Borromean system with three-body interaction

To study quench dynamics beyond two particles we consider a bosonic three-body system ( $N = 3$ ) which is initially noninteracting ( $s = 2$ ) with relative ground-state energy  $E_0 = 1 + s = 3$ . A quench of the *three*-body interaction imposes a sudden change of the  $N$ -body Bethe-Peierls boundary

condition (25) on the hyperradial wave function, while the two-body sector in the hyperangular part  $\Phi(\Omega)$  remains unaffected. This creates a Borromean system with three-body but no two-body interaction, which occurs both in nuclei [45,48] and in ultracold gases [42,49], for instance near a three-body resonance [10].

For the initially noninteracting gas with integer  $s = 2$  the Whittaker  $M$  function (31) is undefined. Instead, one can write the quench solution as a linear combination of the two linearly independent regular solutions  $W_{(1+s)/2, s/2}(-\rho^2)$  and  $W_{-(1+s)/2, s/2}(\rho^2)$ . For noninteger  $s$  the coefficients are fixed by the initial condition  $t \rightarrow 0$  and the boundary condition  $R \rightarrow 0$ , and we recover (36). For integer  $s = 2$ , instead, we obtain the analytical quench solution

$$F(R, t) = e^{-iE_0 t} R^2 e^{-R^2/2} \left[ 1 + \frac{2i}{\pi} \Gamma(-2, \rho^2) \right]. \quad (50)$$

This wave function develops a node at intermediate distance at quarter period  $\omega_0 t = \pi/2$ , in analogy to the  $s = 1/2$  case above. Following the discussion in Sec. IV A, we predict that the three-body contact grows in time as  $C^{(3)}(t) \sim t^4$ . This is consistent with a recent experiment which found that three-body correlations grow slower than two-body ones after an interaction quench [10]. If, instead, three bosons are already resonantly interacting in the two-body sector with  $s = 4.465$  [41] in the initial state before the quench, we expect an anomalous growth law  $C^{(3)}(t) \sim t^{8.93}$  reminiscent of unparticle physics [50,51].

## V. DISCUSSION

In conclusion, we have shown that  $N$ -particle systems quenched to resonant  $N$ -body interaction exhibit scaling dynamics with a complex scale factor, with explicit examples given for  $N = 2, 3$ . This provides a fully analytical form of the nonequilibrium dynamics as the complex scaling of a single negative-energy stationary state. The exact few-body quench dynamics determines also the universal dynamics of a many-body system at times  $t \lesssim \hbar/E_F$  shorter than the many-body timescale where medium effects become important [16].

The complex scaling flow allows us to predict the dynamical scaling of observables after the quench. We find that the integrated two-body contact (12) grows linearly in time at short times after a quench from an ideal to a unitary Fermi gas, with the growth rate  $C(t) \propto (\hbar n/m)t$  proportional to density [9]. This could be observed with state-of-the-art cold atom experiments that measure the two- and three-body contact on very short timescales [5,6,10]. In general, the  $N$ -body contact scales universally as  $C^{(N)}(t) \sim t^{2s}$  after the quench, while the fidelity is anomalously suppressed as  $M(t) = 1 - \gamma |t|^{1+s}$ . For a three-body system where resonant three-body interactions are switched on, this leads to a characteristic scaling with  $s = 2$  (without two-body interaction) or  $s = 4.465$  (resonant two-body interaction in  $l = 0$  state). In our discussion we assumed scale invariance and did not consider Efimov three-body bound states with imaginary  $s = 1.00624i$  that break continuous scale invariance and lead to modulations of the three-body contact [52,53]. Nevertheless, approaching the threshold for three-body bound states provides a way to realize resonant three-body interactions in experiment [10].

Quenches into these states could be a worthwhile topic for future study.

A different question is how an  $N > 2$  particle system evolves after a quench in the two-body interaction. In this case, the quench affects also the hyperangular part of the wave function, and the nonequilibrium evolution might involve several towers of states with the same total angular momentum but different values of  $s$  for their primary states [41,54].

Such strong contact correlations have implications for the description of fluid flow. In general, transport can be described by the Bogoliubov-Born-Green-Kirkwood-Yvon (BBGKY) hierarchy of particle distribution functions where the evolution of the single-particle distribution  $f_1$  depends on the two-particle distribution  $f_2$ , which in turn depends on higher distributions [3]. In a dilute gas, the property of molecular chaos means that particle distributions are uncorrelated and one can set  $f_2 = f_1^2$ : in this way, the hierarchy of equations of motion closes and one can explicitly compute the collision integral in the Boltzmann equation. Our model system is very dilute with an interaction range  $|r_e| \ll n^{-1/3}$  much shorter than the mean particle spacing; at the same time,

however, the strong contact correlations  $g^{(2)}(r, t)$  in Fig. 1 violate molecular chaos  $f_2 \neq f_1^2$  and invalidate a Boltzmann approach formulated solely in terms of the fermionic single-particle distribution but without two-particle pair correlations. Indeed, recent computations of the bulk viscosity [55–60] and thermal conductivity [61] of strongly interacting Fermi gases reveal the importance of contact correlations for transport in extension of the fermionic Boltzmann formulation. The initial buildup of few-body correlations [53,62] should be part of an effective fluid description of quench dynamics.

#### ACKNOWLEDGMENTS

We thank N. Defenu, M. Drescher, J. Maki, J. Thywissen, and W. Zwerger for useful discussions. This work is supported by the Deutsche Forschungsgemeinschaft (German Research Foundation), project-ID 273811115 (SFB1225 ISOQUANT) and under Germany's Excellence Strategy EXC2181/1-390900948 (the Heidelberg STRUCTURES Excellence Cluster).

- 
- [1] T. Schäfer and D. Teaney, Nearly perfect fluidity: From cold atomic gases to hot quark gluon plasmas, *Rep. Prog. Phys.* **72**, 126001 (2009).
  - [2] L. D. Landau and E. M. Lifshitz, *Fluid Mechanics* (Butterworth-Heinemann, Oxford, 1987).
  - [3] H. Smith and H. H. Jensen, *Transport Phenomena* (Oxford University Press, Oxford, 1989).
  - [4] P. Romatschke and U. Romatschke, *Relativistic Fluid Dynamics In and Out of Equilibrium and Applications to Relativistic Nuclear Collisions* (Cambridge University Press, Cambridge, 2019).
  - [5] A. B. Bardon, S. Beattie, C. Luciuk, W. Cairncross, D. Fine, N. S. Cheng, G. J. A. Edge, E. Taylor, S. Zhang, S. Trotzky, and J. H. Thywissen, Transverse demagnetization dynamics of a unitary Fermi gas, *Science* **344**, 722 (2014).
  - [6] C. Luciuk, S. Smale, F. Böttcher, H. Sharum, B. A. Olsen, S. Trotzky, T. Enss, and J. H. Thywissen, Observation of Quantum-Limited Spin Transport in Strongly Interacting Two-Dimensional Fermi Gases, *Phys. Rev. Lett.* **118**, 130405 (2017).
  - [7] M. Knap, A. Shashi, Y. Nishida, A. Imambekov, D. A. Abanin, and E. Demler, Time-Dependent Impurity in Ultracold Fermions: Orthogonality Catastrophe and Beyond, *Phys. Rev. X* **2**, 041020 (2012).
  - [8] M. Cetina, M. Jag, R. S. Lous, I. Fritsche, J. T. M. Walraven, R. Grimm, J. Levinsen, M. M. Parish, R. Schmidt, M. Knap, and E. Demler, Ultrafast many-body interferometry of impurities coupled to a Fermi sea, *Science* **354**, 96 (2016).
  - [9] A. G. Sykes, J. P. Corson, J. P. D’Incao, A. P. Koller, C. H. Greene, A. M. Rey, K. R. A. Hazzard, and J. L. Bohn, Quenching to unitarity: Quantum dynamics in a three-dimensional Bose gas, *Phys. Rev. A* **89**, 021601(R) (2014).
  - [10] R. J. Fletcher, R. Lopes, J. Man, N. Navon, R. P. Smith, M. W. Zwierlein, and Z. Hadzibabic, Two- and three-body contacts in the unitary Bose gas, *Science* **355**, 377 (2017).
  - [11] C. Eigen, J. A. P. Glidden, R. Lopes, E. A. Cornell, R. P. Smith, and Z. Hadzibabic, Universal prethermal dynamics of Bose gases quenched to unitarity, *Nature (London)* **563**, 221 (2018).
  - [12] M. Sun, P. Zhang, and H. Zhai, High Temperature Virial Expansion to Universal Quench Dynamics, *Phys. Rev. Lett.* **125**, 110404 (2020).
  - [13] M. Drescher, M. Salmhofer, and T. Enss, Theory of a resonantly interacting impurity in a Bose-Einstein condensate, *Phys. Rev. Research* **2**, 032011(R) (2020).
  - [14] M. Drescher, M. Salmhofer, and T. Enss, Quench dynamics of the ideal Bose polaron at zero and nonzero temperatures, *Phys. Rev. A* **103**, 033317 (2021).
  - [15] M. G. Skou, T. G. Skov, N. B. Jørgensen, K. K. Nielsen, A. Camacho-Guardian, T. Pohl, G. M. Bruun, and J. J. Arlt, Non-equilibrium quantum dynamics and formation of the Bose polaron, *Nat. Phys.* **17**, 731 (2021).
  - [16] R. Qi, Z. Shi, and H. Zhai, Maximum Energy Growth Rate in Dilute Quantum Gases, *Phys. Rev. Lett.* **126**, 240401 (2021).
  - [17] J. Maki, S. Zhang, and F. Zhou, Dynamics of Strongly Interacting Fermi Gases with Time-Dependent Interactions: Consequence of Conformal Symmetry, *Phys. Rev. Lett.* **128**, 040401 (2022).
  - [18] S. Tan, Energetics of a strongly correlated Fermi gas, *Ann. Phys. (NY)* **323**, 2952 (2008).
  - [19] S. Tan, Large momentum part of a strongly correlated Fermi gas, *Ann. Phys. (NY)* **323**, 2971 (2008).
  - [20] L. P. Pitaevskii and A. Rosch, Breathing modes and hidden symmetry of trapped atoms in two dimensions, *Phys. Rev. A* **55**, R853 (1997).
  - [21] F. Werner and Y. Castin, Unitary gas in an isotropic harmonic trap: Symmetry properties and applications, *Phys. Rev. A* **74**, 053604 (2006).
  - [22] V. Gritsev, P. Barmettler, and E. Demler, Scaling approach to quantum non-equilibrium dynamics of many-body systems, *New J. Phys.* **12**, 113005 (2010).

- [23] E. Balslev and J. M. Combes, Spectral properties of Schrödinger Hamiltonians with dilation analytic potentials, *Commun. Math. Phys.* **22**, 280 (1971).
- [24] M. Reed and B. Simon, *Methods of Modern Mathematical Physics: Analysis of Operators* (Academic Press, San Diego, 1978), Vol. 4.
- [25] V. Bach, J. Fröhlich, and I. M. Sigal, Quantum electrodynamics of confined nonrelativistic particles, *Adv. Math.* **137**, 299 (1998).
- [26] T. Busch, B.-G. Englert, K. Rzazewski, and M. Wilkens, Two cold atoms in a harmonic trap, *Found. Phys.* **28**, 549 (1998).
- [27] A. D. Kerin and A. M. Martin, Two-body quench dynamics of harmonically trapped interacting particles, *Phys. Rev. A* **102**, 023311 (2020).
- [28] L. M. A. Kehrberger, V. J. Bolsinger, and P. Schmelcher, Quantum dynamics of two trapped bosons following infinite interaction quenches, *Phys. Rev. A* **97**, 013606 (2018).
- [29] Y. Nishida and D. T. Son, Nonrelativistic conformal field theories, *Phys. Rev. D* **76**, 086004 (2007).
- [30] F. Werner and Y. Castin, General relations for quantum gases in two and three dimensions. two-component fermions, *Phys. Rev. A* **86**, 013626 (2012).
- [31] S. Moroz, Scale-invariant Fermi gas in a time-dependent harmonic potential, *Phys. Rev. A* **86**, 011601(R) (2012).
- [32] M. M. Parish and J. Levinsen, Quantum dynamics of impurities coupled to a Fermi sea, *Phys. Rev. B* **94**, 184303 (2016).
- [33] T. Schäfer and C. Chafin, Scaling flows and dissipation in the dilute fermi gas at unitarity, in *The BCS-BEC Crossover and the Unitary Fermi Gas*, edited by W. Zwerger (Springer, Berlin, 2012), Chap. 10, p. 375.
- [34] J. Berges, A. Rothkopf, and J. Schmidt, Nonthermal Fixed Points: Effective Weak Coupling for Strongly Correlated Systems Far from Equilibrium, *Phys. Rev. Lett.* **101**, 041603 (2008).
- [35] P. A. Murthy, N. Defenu, L. Bayha, M. Holten, P. M. Preiss, T. Enss, and S. Jochim, Quantum scale anomaly and spatial coherence in a 2D Fermi superfluid, *Science* **365**, 268 (2019).
- [36] M. Olshanii, H. Perrin, and V. Lorent, Example of a Quantum Anomaly in the Physics of Ultracold Gases, *Phys. Rev. Lett.* **105**, 095302 (2010).
- [37] J. Hofmann, Quantum Anomaly, Universal Relations, and Breathing Mode of a Two-Dimensional Fermi Gas, *Phys. Rev. Lett.* **108**, 185303 (2012).
- [38] M. Holten, L. Bayha, A. C. Klein, P. A. Murthy, P. M. Preiss, and S. Jochim, Anomalous Breaking of Scale Invariance in a Two-Dimensional Fermi Gas, *Phys. Rev. Lett.* **121**, 120401 (2018).
- [39] T. Pepler, P. Dyke, M. Zamorano, I. Herrera, S. Hoinka, and C. J. Vale, Quantum Anomaly and 2D-3D Crossover in Strongly Interacting Fermi Gases, *Phys. Rev. Lett.* **121**, 120402 (2018).
- [40] M. Syed, T. Enss, and N. Defenu, Dynamical quantum phase transition in a bosonic system with long-range interactions, *Phys. Rev. B* **103**, 064306 (2021).
- [41] D. Blume, Few-body physics with ultracold atomic and molecular systems in traps, *Rep. Prog. Phys.* **75**, 046401 (2012).
- [42] Y. Nishida, D. T. Son, and S. Tan, Universal Fermi Gas with Two- and Three-Body Resonances, *Phys. Rev. Lett.* **100**, 090405 (2008).
- [43] L. Pricoupenko, Modeling Interactions for Resonant  $p$ -Wave Scattering, *Phys. Rev. Lett.* **96**, 050401 (2006).
- [44] L. Pricoupenko, Pseudopotential in resonant regimes, *Phys. Rev. A* **73**, 012701 (2006).
- [45] M. V. Zhukov, B. V. Danilin, D. Fedorov, J. M. Bang, I. J. Thompson, and J. S. Vaagen, Bound state properties of Borromean halo nuclei:  ${}^6\text{He}$  and  ${}^{11}\text{Li}$ , *Phys. Rep.* **231**, 151 (1993).
- [46] Y. Castin and F. Werner, The unitary gas and its symmetry properties, in *The BCS-BEC Crossover and the Unitary Fermi Gas*, edited by W. Zwerger (Springer, Berlin, 2012), Chap. 5, p. 127.
- [47] T. Enss and R. Haussmann, Quantum Mechanical Limitations to Spin Diffusion in the Unitary Fermi Gas, *Phys. Rev. Lett.* **109**, 195303 (2012).
- [48] M. Hongo and D. T. Son, Universal Properties of Weakly Bound Two-Neutron Halo Nuclei, *Phys. Rev. Lett.* **128**, 212501 (2022).
- [49] W. Zwerger, Quantum-unbinding near a zero temperature liquid-gas transition, *J. Stat. Mech.* (2019) 103104.
- [50] H. Georgi, Unparticle Physics, *Phys. Rev. Lett.* **98**, 221601 (2007).
- [51] H.-W. Hammer and D. T. Son, Unnuclear physics: Conformal symmetry in nuclear reactions, *Proc. Natl. Acad. Sci. USA* **118**, e2108716118 (2021).
- [52] V. E. Colussi, J. P. Corson, and J. P. D’Incao, Dynamics of Three-Body Correlations in Quenched Unitary Bose Gases, *Phys. Rev. Lett.* **120**, 100401 (2018).
- [53] V. E. Colussi, B. E. van Zwol, J. P. D’Incao, and S. J. J. M. F. Kokkelmans, Bunching, clustering, and the buildup of few-body correlations in a quenched unitary Bose gas, *Phys. Rev. A* **99**, 043604 (2019).
- [54] V. Bekassy and J. Hofmann, Nonrelativistic Conformal Invariance in Mesoscopic Two-Dimensional Fermi Gases, *Phys. Rev. Lett.* **128**, 193401 (2022).
- [55] K. Dusling and T. Schäfer, Bulk Viscosity and Conformal Symmetry Breaking in the Dilute Fermi Gas near Unitarity, *Phys. Rev. Lett.* **111**, 120603 (2013).
- [56] T. Enss, Bulk Viscosity and Contact Correlations in Attractive Fermi Gases, *Phys. Rev. Lett.* **123**, 205301 (2019).
- [57] Y. Nishida, Viscosity spectral functions of resonating fermions in the quantum virial expansion, *Ann. Phys. (NY)* **410**, 167949 (2019).
- [58] J. Hofmann, High-temperature expansion of the viscosity in interacting quantum gases, *Phys. Rev. A* **101**, 013620 (2020).
- [59] K. Fujii and Y. Nishida, Bulk viscosity of resonating fermions revisited: Kubo formula, sum rule, and the dimer and high-temperature limits, *Phys. Rev. A* **102**, 023310 (2020).
- [60] J. Maki and S. Zhang, Role of Effective Range in the Bulk Viscosity of Resonantly Interacting  $s$ - and  $p$ -Wave Fermi Gases, *Phys. Rev. Lett.* **125**, 240402 (2020).
- [61] B. Frank, W. Zwerger, and T. Enss, Quantum critical thermal transport in the unitary Fermi gas, *Phys. Rev. Research* **2**, 023301 (2020).
- [62] S. Musolino, H. Kurkjian, M. Van Regemortel, M. Wouters, S. J. J. M. F. Kokkelmans, and V. E. Colussi, Bose-Einstein Condensation of Efimovian Triples in the Unitary Bose Gas, *Phys. Rev. Lett.* **128**, 020401 (2022).